

CRYSTAL CHEMISTRY OF TRIOCTAHEDRAL MICAS-1M FROM THE ALTO PARANAÍBA IGNEOUS PROVINCE, SOUTHEASTERN BRAZIL

MARIA FRANCA BRIGATTI[§]

Dipartimento di Scienze della Terra dell'Università di Modena e Reggio Emilia, Via S. Eufemia, 19, I-41100 Modena, Italy

LUCA MEDICI[§]

IRA – CNR, Area della Ricerca di Potenza, Via S. Loja, I-85050 Tito Scalo (PZ), Italy

LUCIANO POPPI

Dipartimento di Scienze della Terra dell'Università di Modena e Reggio Emilia, Via S. Eufemia, 19, I-41100 Modena, Italy

CARMELA VACCARO[§]

Dipartimento di Scienze della Terra dell'Università di Ferrara, C.so Ercole I d'Este, 32, I-44100 Ferrara, Italy

ABSTRACT

The crystal structures of nine trioctahedral mica-1M crystals (phlogopite and ferroan phlogopite containing Fe³⁺ in tetrahedral position, ferroan tetra-ferriphlogopite, and titanian phlogopite), from ultramafic alkaline-silicate lavas and alkaline-silicate, silicate-carbonatite and carbonatite plutonic rocks occurring in the Alto Paranaíba Igneous Province (southeastern Brazil), were refined from single-crystal X-ray data in the space group *C2/m* to *R* values between 0.025 and 0.039. These mica crystals are characterized by low to very low Al content; therefore, Fe³⁺ may be essential to fill the tetrahedral site. The octahedral position of all the crystals studied is characterized by variable amounts of Fe²⁺, Fe³⁺ and Ti⁴⁺ in substitution for Mg. The two independent octahedral sites, *M1* and *M2*, show equivalent mean electron-density and mean bond-distances in most cases. Order at the octahedral sites is enhanced in the Ti-rich crystal from Presidente Olegario owing to the preference of Ti for the *M2* site. The lateral parameters *a* and *b* reflect variations in tetrahedron composition, whereas the periodicity along *c* depends on octahedron composition. The crystal-chemical features of these micas are controlled by the peculiar composition of the rocks, by the high *f*(O₂), *a*(H₂O), and *f*(CO₂), and by metasomatic events that have affected the Alto Paranaíba Igneous Province.

Keywords: phlogopite, tetra-ferriphlogopite, crystal structure, chemical composition, Alto Paranaíba, Brazil.

SOMMAIRE

Nous avons affiné la structure cristalline de neuf échantillons de mica-1M trioctaédrique (phlogopite et phlogopite ferreuse contenant le Fe³⁺ en position tétraédrique, tétra-ferriphlogopite ferreuse, et phlogopite titanifère), provenant de laves silicatées ultramafiques et alcalines, et de roches plutoniques silicatées alcalines, silicatées et carbonatitiques, et carbonatitiques faisant partie de la province ignée de Alto Paranaíba, dans le sud-est du Brésil; les affinements ont été effectués sur cristaux uniques dans le groupe spatial *C2/m*, et ont mené à un résidu *R* entre 0.025 et 0.039. Ces cristaux de mica possèdent une déficience plus ou moins marquée en Al; le Fe³⁺ est donc essentiel dans certains cas pour combler le site tétraédrique. La position octaédrique de tous les cristaux étudiés contient des proportions variables de Fe²⁺, Fe³⁺ et Ti⁴⁺ en substitution au Mg. Deux sites octaédriques indépendants, *M1* et *M2*, font preuve d'une distribution moyenne d'électrons et de longueurs de liaisons équivalentes dans la plupart des cas. En revanche, une mise en ordre est caractéristique du cristal riche en Ti de la coulée de Presidente Olegario, à cause de la préférence du Ti pour le site *M2*. Les paramètres latéraux du feuillet, *a* et *b*, dépendent des variations en cations logés dans les tétraèdres, tandis que la périodicité le long de *c* dépend plutôt de la population de cations dans le site octaédrique. Les caractéristiques cristalochimiques des échantillons de mica de cette suite sont régies par la composition particulière des roches, ainsi que par les valeurs élevées de *f*(O₂), *a*(H₂O), et *f*(CO₂), et les événements de métasomatose qui ont affectés les roches de la province ignée de Alto Paranaíba.

(Traduit par la Rédaction)

Mots-clés: phlogopite, tétra-ferriphlogopite, structure cristalline, composition chimique, Alto Paranaíba, Brésil.

[§] *E-mail addresses:* brigatti@unimo.it, medici@ira.pz.cnr.it, vcr@dns.unife.it

INTRODUCTION

Micas from the ultramafic alkaline and alkaline-carbonatite rocks in the Alto Paranaíba Igneous Province, Brazil (APIP, Gibson *et al.* 1995) show a remarkable variation in chemical composition. They are mostly phlogopite with variable Fe/(Fe + Mg) values and Ti contents (Gaspar 1989); in some cases, there is a deficiency of (Al + Si) in the tetrahedral site, which results in the presence of tetrahedrally coordinated Fe³⁺ and, therefore, a significant contribution of the tetra-ferriphlogopite end member. There have been many attempts, based on chemical composition, to determine the relative proportion of end members (*i.e.*, phlogopite, annite and tetra-ferriphlogopite) and to use those proportions both to discriminate among different alkaline rock-types and to establish evolutionary trends of mica. The strong influence that mica composition plays on igneous processes in the APIP province thus accounts for the broad interest in this igneous province (*e.g.*, Gaspar & Wyllie 1987, Araújo & Gaspar 1993, Gaspar *et al.* 1994, Gibson *et al.* 1995, Brigatti *et al.* 1996b, Brod *et al.* 2000, 2001).

Some investigations (Brigatti *et al.* 1996a, b, and references therein, 1999, Giuli *et al.* 2001) have focused on micas from the Tapira carbonatite complex and focused on the crystal chemistry and structure in its relationships with several issues such as the conditions of mica crystallization, the relationships between structure and oxidation state of iron, both in tetrahedral and octa-

hedral sites, and the local environment of iron in tetra-ferriphlogopite.

This work deals with the crystal chemistry of nine crystals of trioctahedral mica from the Alto Paranaíba Igneous Province whose chemical composition involves phlogopite, annite and tetra-ferriphlogopite end members. Crystals were collected in various units of the Tapira layered intrusive complex, and in ultramafic rocks of Limeira (kamafugitic intrusion) and Presidente Olegario (kamafugitic lavas).

The aims of this work are: 1) to investigate the crystal chemistry and the degree of order of octahedrally coordinated cations in micas from igneous rocks derived from the same primary magma, 2) to compare the crystal-chemical features and the geometrical distortions of ferroan tetra-ferriphlogopite and those of tetra-ferriphlogopite previously reported (Semenova *et al.* 1977, Hazen *et al.* 1981, Brigatti *et al.* 1996a, b, 1999), and 3) to assess crystal-chemical differences between ⁶Fe²⁺-rich trioctahedral micas of this study and those reported by Brigatti *et al.* (1996b), who considered ⁶Fe²⁺-poor phlogopite from Tapira complex, and therefore crystals derived from a less evolved magma.

THE BODIES SAMPLED

The trioctahedral micas studied occur in ultramafic rocks of the Alto Paranaíba Igneous Province, southeastern Brazil, and were sampled in Presidente Olegario, Limeira I and Tapira areas (Table 1). The region around Presidente Olegario appears to have been the site of many volcanic centers, from which thick sequences of lavas and tuffs of kamafugitic composition erupted (Gibson *et al.* 1995). The trioctahedral micas have a high Ti content. Limeira I is an elongate ultramafic intrusion, containing dunite, harzburgite and spinel lherzolite xenoliths. This intrusion, previously referred to as kimberlite, is actually classified as kamafugite owing to the Ca and Ti content of the rocks (Gibson *et al.* 1995). Finally, the Tapira plutonic complex consists dominantly of bebedourite, a plutonic rock formed mainly of diopsidic pyroxene and variable amount of phlogopite, perovskite, apatite, magnetite, titanian garnet and rare titanite, with subordinate amounts of carbonatite, serpentinite (dunite), syenite and ultramafic ultrapotassic dykes (Gibson *et al.* 1995, Brod *et al.* 2001).

EXPERIMENTAL METHODS

Chemical determinations

The major-element analyses of nine samples of ⁴Fe³⁺-containing phlogopite, ferroan ⁴Fe³⁺-containing phlogopite, ferroan tetra-ferriphlogopite and titanian phlogopite were carried out using a wavelength-dispersion ARL-SEMQ electron microprobe. The microprobe was operated at an accelerating voltage of 15 kV, a sample current of 15 nA, and an enlarged spot size of

TABLE 1. SAMPLES, ROCK TYPES, LOCALITIES, AND MINERALS ASSOCIATED WITH THE TRIOCTAHEDRAL MICAS FROM THE ALTO PARANAÍBA IGNEOUS PROVINCE, BRAZIL

| Sample | Occurrence | Paragenesis |
|----------|---|--|
| Tpp16-6 | Garnet magnetitite Tapira complex | Cumulus phases: Grt, Prv, Mgt Intercumulus phases: Cpx, Phl, Tfp, Ap, carbonates |
| Tax27-1 | Clinopyroxenite Tapira complex | Cumulus phases: Cpx, Prv Intercumulus phases: Ap, Phl, Cal, Ilm, titaniferous Mgt |
| Taa11-1A | Bebedourite Tapira complex | Cumulus phases: Cpx, Phl Intercumulus phases: Ap, Prv, Mgt, carbonates |
| Tai17-1 | Bebedourite Tapira complex | Cumulus phases: Cpx, Phl Intercumulus phases: Ap, Prv, Mgt, carbonates |
| Ta9 | Garnet magnetitite Tapira complex | Cumulus phases: Grt, Prv, Mgt Intercumulus phases: Cpx, Phl, Ap, carbonates |
| Li12a | Kamafugite Limeira diatreme | Cpx, Phl, Ilm, Ol |
| Ma1 | Kamafugite Presidente Olegario lavas | Phl, Di, Amp, Ol, Prv, Mgt |

Symbols: Amp amphibole, Ap apatite, Cal calcite, Cpx clinopyroxene, Di diopside, Grt garnet, Ilm ilmenite, Mgt magnetite, Ol olivine, Phl phlogopite, Prv perovskite, Tfp tetra-ferriphlogopite.

about 8 μm to minimize beam-induced damage to the mineral. Analyses and data reductions were performed using the Probe software package of Donovan (1995). The determination of fluorine content was carried out following the indications of Foley (1989). The Ti and Ba contents were corrected for overlap of $\text{TiK}\alpha$ and $\text{BaK}\alpha$ peaks. The following standards were used for the determination of mica composition: fluorite (F), microcline (K), albite (Na), spessartine (Al, Mn), ilmenite (Fe, Ti), clinopyroxene (Si, Ca), olivine (Mg), paracelsian (Ba).

The calculation of a chemical formula of a mica is problematic because of the wide variety of chemical substitutions (cationic and anionic), disorder within the structure, the unknown oxidation state of cations and site vacancies. Chemical formulae were therefore obtained using two different schemes of calculation. The first scheme was applied to crystals analyzed on pol-

ished thin sections and involved the following procedure for normalization: i) the positive charges were balanced on 10 oxygen atoms and $2(\text{OH} + \text{F} + \text{Cl})$ atoms. ii) Tetrahedral sites were considered completely filled by Si and Al to an occupancy of exactly 4. Only where the sum $\text{Si} + \text{Al}$ fell short of 4 atoms per formula unit (*apfu*) was Fe^{3+} considered to occupy the tetrahedral position. iii) The octahedral sites were filled with Mg, Fe, Ti, and Mn, whereas iv) Na, K, Ca, and Ba were assigned to the interlayer positions. The values obtained are shown in Figures 1 and 2.

A second scheme of calculation was used to obtain the chemical formulae of crystals used in the structure refinement (Table 2). Compositions reported in Table 2 were obtained by combining the results of: i) the average result of at least six microprobe point-analyses of the same crystal used in the structure refinement; ii) $(\text{OH})^-$ determination on several crystals from the same sample that yielded the crystal used for the structure refinement; $(\text{OH})^-$ was measured by thermogravimetric analysis in He gas flow to minimize the reaction $2\text{FeO} + 2(\text{OH})^- \rightarrow \text{Fe}_2\text{O}_3 + \text{H}_2 + \text{O}^{2-}$, using a Seiko SSC 5200 thermal analyzer (heating rate $10^\circ\text{C}/\text{min}$ and flow rate $200 \text{ mL}/\text{min}$), equipped with a mass spectrometer (GeneSys ESS Quadstar 422); iii) the amount of Fe^{2+} (estimated standard deviation $\sigma < 4\%$) was determined by a semi-microvolumetric method (Meyrowitz 1970). The consistency and accuracy of the experimental $(\text{OH})^-$ and Fe^{2+} content were checked by a best-fit calculation using structural parameters of about 200 refined crystals reported in literature (Brigatti & Guggenheim 2000). The chemical formulae were based on $\text{O}_{12-x-y-z}$, where x is the proportion of $(\text{OH})^-$ groups per formula unit, y is F in *apfu*, and z is Cl in *apfu* (atoms per formula unit).

TABLE 2. CHEMICAL COMPOSITION OF THE CRYSTALS OF TRIOCTAHEDRAL MICA-1M STUDIED

| | Tpp16 -6a | Tax27 -1 | Taa11 -1A | Tai17 -1 | Ta9 | Li12a | Tpp16 -6b | Tpp16 -6c | Ma1 |
|---|--------------|-------------|--------------|-------------|--------|--------|--------------|--------------|--------|
| SiO_2 , wt% | 39.50 | 40.12 | 38.68 | 38.57 | 39.10 | 41.55 | 39.17 | 38.92 | 39.91 |
| TiO_2 | 1.06 | 1.38 | 1.81 | 1.68 | 1.52 | 0.98 | 0.17 | 0.19 | 6.00 |
| Al_2O_3 | 12.35 | 9.11 | 13.20 | 12.78 | 10.00 | 10.82 | 0.75 | 0.69 | 12.22 |
| Fe_2O_3 | 4.01 | 5.84 | 1.41 | 3.13 | 1.65 | 1.27 | 15.77 | 15.77 | 0.51 |
| FeO | 2.20 | 7.02 | 9.70 | 7.24 | 17.79 | 7.25 | 9.33 | 9.33 | 5.72 |
| MgO | 25.61 | 21.82 | 20.37 | 21.67 | 15.19 | 23.26 | 20.54 | 20.65 | 18.84 |
| MnO | 0.06 | 0.15 | 0.21 | 0.10 | 0.57 | 0.00 | 0.14 | 0.09 | 0.03 |
| CaO | 0.00 | 0.00 | 0.03 | 0.00 | 0.00 | 0.00 | 0.00 | 0.40 | 0.00 |
| BaO | 0.00 | 0.00 | 0.00 | 0.32 | 0.52 | 0.00 | 0.19 | 0.21 | 0.55 |
| Na_2O | 0.07 | 0.18 | 0.13 | 0.17 | 0.02 | 0.26 | 0.03 | 0.00 | 0.14 |
| K_2O | 10.71 | 10.17 | 10.50 | 10.49 | 10.04 | 10.27 | 10.16 | 9.88 | 10.34 |
| H_2O | 3.95 | 4.00 | 3.75 | 3.85 | 3.55 | 3.55 | 3.70 | 3.70 | 1.75 |
| F | 0.48 | 0.21 | 0.21 | 0.00 | 0.05 | 0.79 | 0.05 | 0.17 | 3.99 |
| Sum | 100.00 | 100.00 | 100.00 | 100.00 | 100.00 | 100.00 | 100.00 | 100.00 | 100.00 |
| Unit-cell content recalculated on the basis of $\text{O}_{(12-x-y-z)}$, $(\text{OH})^-$, F _y | | | | | | | | | |
| Si <i>apfu</i> | 2.82 | 2.94 | 2.84 | 2.82 | 3.00 | 3.01 | 3.03 | 3.02 | 2.94 |
| Al | 1.04 | 0.78 | 1.14 | 1.10 | 0.90 | 0.92 | 0.07 | 0.06 | 1.06 |
| Fe^{3+} | 0.14 | 0.28 | 0.02 | 0.08 | 0.10 | 0.07 | 0.90 | 0.92 | 0.00 |
| Sum | 4.00 | 4.00 | 4.00 | 4.00 | 4.00 | 4.00 | 4.00 | 4.00 | 4.00 |
| Ti | 0.06 | 0.08 | 0.10 | 0.09 | 0.09 | 0.05 | 0.01 | 0.01 | 0.33 |
| Fe^{3+} | 0.08 | 0.04 | 0.06 | 0.10 | 0.00 | 0.00 | 0.01 | 0.00 | 0.03 |
| Fe^{2+} | 0.13 | 0.43 | 0.60 | 0.44 | 1.14 | 0.44 | 0.60 | 0.60 | 0.35 |
| Mg | 2.73 | 2.39 | 2.23 | 2.36 | 1.73 | 2.51 | 2.36 | 2.38 | 2.07 |
| Mn | 0.00 | 0.01 | 0.01 | 0.01 | 0.04 | 0.00 | 0.01 | 0.01 | 0.00 |
| Sum | 3.00 | 2.95 | 3.00 | 3.00 | 3.00 | 3.00 | 2.99 | 3.00 | 2.78 |
| Na | 0.01 | 0.03 | 0.02 | 0.02 | 0.00 | 0.04 | 0.00 | 0.00 | 0.02 |
| K | 0.98 | 0.95 | 0.98 | 0.98 | 0.98 | 0.95 | 1.00 | 0.97 | 0.97 |
| Ca | 0.00 | 0.00 | 0.00 | 0.00 | 0.00 | 0.00 | 0.00 | 0.03 | 0.00 |
| Ba | 0.00 | 0.00 | 0.00 | 0.01 | 0.02 | 0.00 | 0.01 | 0.01 | 0.02 |
| Sum | 0.99 | 0.98 | 1.00 | 1.01 | 1.00 | 0.99 | 1.01 | 1.01 | 1.01 |
| OH | 1.88 | 1.95 | 1.84 | 1.88 | 1.82 | 1.71 | 1.91 | 1.91 | 0.86 |
| F | 0.11 | 0.05 | 0.05 | 0.00 | 0.01 | 0.18 | 0.01 | 0.04 | 0.93 |
| O | 10.01 | 10.00 | 10.11 | 10.12 | 10.17 | 10.11 | 10.08 | 10.05 | 10.21 |
| Sum | 12.00 | 12.00 | 12.00 | 12.00 | 12.00 | 12.00 | 12.00 | 12.00 | 12.00 |

Note: Labels a, b, c refer to different crystals from the same rock sample. Nature of the trioctahedral micas: Tpp16-6a: $^{19}\text{Fe}^{3+}$ -bearing phlogopite, Tax27-1, Taa11-1A, Tai17-1, Ta9 and Li12a: ferroan $^{19}\text{Fe}^{3+}$ -bearing phlogopite; Tpp16-6b, Tpp16-6c: ferroan tetra-ferriphlogopite; Ma1: titanian phlogopite. *apfu*: atoms per formula unit.

Single-crystal X-ray-diffraction data

Single-crystal precession photographs were taken of several crystals selected from the same crushed rock sample. To determine the cell dimensions and to collect intensity data, the best crystal found in each sample was mounted onto a Siemens P4P rotating-anode, fully automated, four-circle diffractometer operating at 50 kV and 140 mA with graphite-monochromatized $\text{MoK}\alpha$ radiation ($\gamma = 0.71073 \text{ \AA}$), equipped with XSCANS software (Siemens 1993, User Manual). A set of over 40 reflections was used to refine the unit-cell parameters (Table 3). Intensities were measured up to $2\theta = 70.0^\circ$ ($1 \leq h \leq 8$, $14 \leq k \leq 14$, $15 \leq l \leq 15$) using a ω -scan mode (window width from 1.4 to 3.0°), with scan speeds inversely proportional to intensity, varying from 1 to $10^\circ/\text{minute}$. The intensities and position of three standard reflections were checked every 100 reflections to monitor stability of the crystal and instrument. Information relevant to data collection and structure determination is given in Table 3. For the absorption correction, 10 to 15 intense diffraction-maxima in the 2θ range from

TABLE 3. DETAILS OF THE X-RAY DATA COLLECTION, STRUCTURE REFINEMENT AND UNIT-CELL PARAMETERS FOR THE CRYSTALS OF TRIOCTAHEDRAL MICA-1M STUDIED

| Samples | Dimensions (mm) | N_{obs} | $R_{\text{sym}} \times 100$ | $R_{\text{obs}} \times 100$ | a (Å) | b (Å) | c (Å) | β (°) | V (Å ³) |
|----------|--------------------|------------------|-----------------------------|-----------------------------|-----------|-----------|-----------|-------------|-----------------------|
| Tpp16-6a | 0.14 × 0.14 × 0.01 | 645 | 3.4 | 3.3 | 5.330(1) | 9.239(1) | 10.305(1) | 99.89(1) | 499.9 |
| Tax27-1 | 0.16 × 0.16 × 0.04 | 625 | 2.5 | 2.6 | 5.351(1) | 9.267(2) | 10.311(1) | 99.99(1) | 503.5 |
| Taa11-1A | 0.52 × 0.44 × 0.02 | 626 | 2.4 | 3.6 | 5.329(2) | 9.244(2) | 10.271(3) | 99.97(2) | 498.3 |
| Tai17-1 | 0.26 × 0.16 × 0.02 | 669 | 1.9 | 2.5 | 5.3355(8) | 9.2457(7) | 10.294(2) | 99.94(1) | 500.2 |
| Ta9 | 0.14 × 0.12 × 0.01 | 532 | 3.2 | 2.8 | 5.344(1) | 9.259(2) | 10.280(2) | 100.01(1) | 500.9 |
| Lil2a | 0.14 × 0.09 × 0.01 | 774 | 2.2 | 3.9 | 5.331(1) | 9.227(1) | 10.275(2) | 99.96(2) | 497.8 |
| Tpp16-6b | 0.10 × 0.10 × 0.02 | 678 | 2.6 | 2.8 | 5.360(1) | 9.293(1) | 10.314(2) | 100.01(1) | 505.9 |
| Tpp16-6c | 0.22 × 0.20 × 0.03 | 934 | 2.5 | 2.5 | 5.3637(5) | 9.2908(8) | 10.321(1) | 99.995(9) | 506.5 |
| Ma1 | 0.16 × 0.10 × 0.01 | 827 | 3.4 | 2.9 | 5.317(1) | 9.208(2) | 10.118(2) | 100.15(1) | 487.6 |

Labels a, b, c refer to different crystals from the same rock sample. Standard deviations are given in parentheses.

$$R_{\text{sym}} = \sum_{hkl} \sum_{i=1}^n |I_{hkl} - \bar{I}_{hkl}| / \sum_{hkl} \sum_{i=1}^n I_{hkl}$$

10° to 60° were chosen for Ψ diffraction-vector scans (from 0° to 360° at 10° ϕ intervals) following the method of North *et al.* (1968). Intensity data were then corrected for absorption and Lorentz-polarization effects. The equivalent pairs were averaged, and the resulting discrepancy-factors were calculated ($0.019 \leq R_{\text{sym}} \leq 0.034$; Table 3). The refinements were performed in the space group $C2/m$ using the ORFLS least-squares program (Busing *et al.* 1962) on $I \geq 3\sigma(I)$ reflections (Table 3).

Atom-position parameters from Brigatti *et al.* (1996b) for the space group $C2/m$ were used as the initial values for all refinements. Fully ionized scattering factors were used for octahedral M and interlayer A sites, whereas mixed scattering factors were assumed for anion and tetrahedral sites. At the final stage of refinement, a complete difference-Fourier electron density (DED) map was calculated. Table 4 contains complete sets of the final positional and equivalent isotropic and anisotropic displacement parameters; Tables 5 and 6 list selected interatomic distances and parameters obtained from structure refinements, respectively. To obtain the site-occupancies of $M1$ and $M2$, the refined structural parameters and the results of electron-microprobe data were treated by a minimization procedure (based on the function FMINS predefined in the MATLAB program library: Moler 1992). Procedural details are reported in Brigatti *et al.* (2000). Refined and calculated site-occupancies are reported in Table 7. Tables of observed and calculated structure-factors are available at the Depository of Unpublished Data, CISTI, National Research Council, Ottawa, Ontario K1A 0S2, Canada.

RESULTS AND DISCUSSION

Chemical composition

The variation in composition of trioctahedral micas-1M from the Alto Paranaíba Igneous Province is re-

ported in Figures 1 and 2. Both Al and Fe^{3+} replace Si; the ratio Fe^{3+} (or $\text{Fe}^{3+} + \text{Al}$) : Si is equal to 1 : 3 and the ratio Al (or Al + Fe) : Si is equal to 1.2 : 2.8. A nearly complete solid-solution exists in this site between phlogopite and tetra-ferriphlogopite. Mg, Fe and Ti represent the main octahedrally coordinated cations. The level of Ti increases from micas that occur in the Tapira Complex to micas that occur in the Presidente Olegario lavas. The composition of phlogopite from Limeira I ($0 \leq {}^{[4]}\text{Fe} \leq 0.34$, $0 \leq {}^{[6]}\text{Fe} \leq 0.24$, $2.52 \leq {}^{[4]}\text{Si} \leq 2.96$, $0.77 \leq {}^{[4]}\text{Al} \leq 1.48$; $0.65 \leq {}^{[6]}\text{Mg} \leq 2.78$, $0.05 \leq {}^{[6]}\text{Ti} \leq 0.23$, $0 \leq {}^{[6]}\text{Mn} \leq 0.03$ *apfu*) approaches that of phlogopite from the Tapira Complex. The composition is very close to that of phlogopite from bebedourite (Brigatti *et al.* 1996b), whereas phlogopite from Presidente Olegario lavas shows a quite different composition characterized by lower Fe and higher Ti contents ($0.14 \leq {}^{[4]}\text{Fe} \leq 0.30$, $0 \leq {}^{[6]}\text{Fe} \leq 0.07$, $2.79 \leq {}^{[4]}\text{Si} \leq 3.02$, $0.70 \leq {}^{[4]}\text{Al} \leq 1.07$, $2.00 \leq {}^{[6]}\text{Mg} \leq 2.19$, $0.33 \leq {}^{[6]}\text{Ti} \leq 0.41$, $0 \leq {}^{[6]}\text{Mn} \leq 0.01$ *apfu*). Crystals from the Tapira Complex are characterized by marked variability among rock types: i) the composition of trioctahedral micas from dunitites approaches end-member phlogopite ($2.82 \leq {}^{[4]}\text{Si} \leq 2.84$; $1.07 \leq {}^{[4]}\text{Al} \leq 1.09$, $0.08 \leq {}^{[4]}\text{Fe} \leq 0.11$, $2.62 \leq {}^{[6]}\text{Mg} \leq 2.67$, $0.21 \leq {}^{[6]}\text{Fe} \leq 0.25$, $0.05 \leq {}^{[6]}\text{Ti} \leq 0.06$, ${}^{[6]}\text{Mn} = 0$; Brigatti *et al.* 1996b). ii) Unlike phlogopite from dunitites, phlogopite from clinopyroxenites is rich in iron, both in tetrahedral and in octahedral sites ($2.83 \leq {}^{[4]}\text{Si} \leq 2.89$, $0.76 \leq {}^{[4]}\text{Al} \leq 0.79$, $0.34 \leq {}^{[4]}\text{Fe} \leq 0.38$, $2.25 \leq {}^{[6]}\text{Mg} \leq 2.38$, $0.39 \leq {}^{[6]}\text{Fe} \leq 0.45$, $0.07 \leq {}^{[6]}\text{Ti} \leq 0.08$, $0.01 \leq {}^{[6]}\text{Mn} \leq 0.02$ *apfu*). iii) The occupancy of octahedra in micas from bebedourite varies widely ($1.79 \leq {}^{[6]}\text{Mg} \leq 2.63$, $0.22 \leq {}^{[6]}\text{Fe} \leq 0.74$, $0.08 \leq {}^{[6]}\text{Ti} \leq 0.18$, $0 \leq {}^{[6]}\text{Mn} \leq 0.02$ *apfu*), and Si is replaced by tetrahedrally coordinated Al (or Fe^{3+}) to maintain the charge balance ($2.55 \leq {}^{[4]}\text{Si} \leq 2.82$, $1.04 \leq {}^{[4]}\text{Al} \leq 1.23$, $0.04 \leq {}^{[4]}\text{Fe} \leq 0.25$ *apfu*). iv) In garnet magnetite rocks, the composition of the trioctahedral mica varies from phlogopite to tetra-ferriphlo-

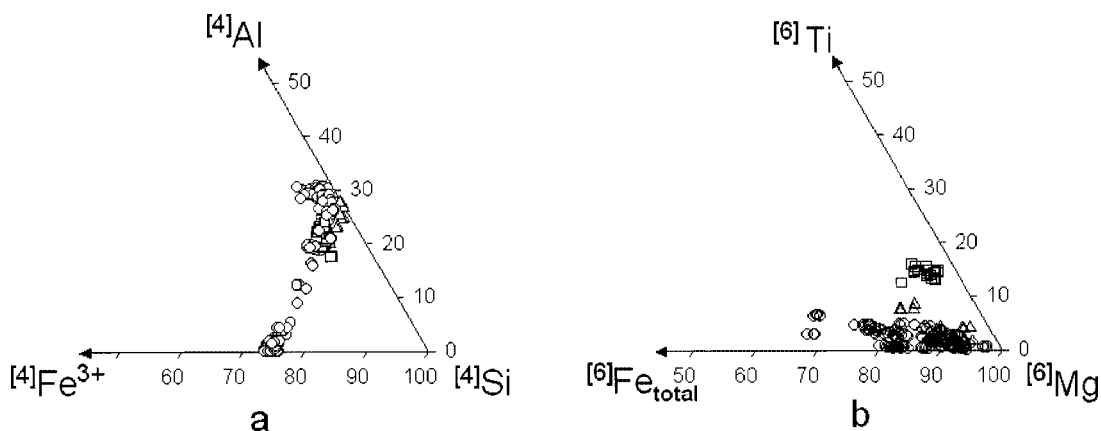


FIG. 1. Proportion of Si, Al and Fe^{3+} at a) the tetrahedral site, and b) the octahedral site in trioctahedral micas from the Alto Paranaíba Igneous Province. Symbols: circles: mica crystals from the Tapira Complex, triangles: mica crystals from the Limeira I intrusion, and squares: mica crystals from the Presidente Olegario lavas.

gopite ($2.77 \leq [^4]\text{Si} \leq 3.01$, $0.01 \leq [^4]\text{Al} \leq 1.12$, $0.06 \leq [^4]\text{Fe} \leq 0.99$, $1.74 \leq [^6]\text{Mg} \leq 2.66$, $0.19 \leq [^6]\text{Fe} \leq 0.78$, $0 \leq [^6]\text{Ti} \leq 0.11$, $0 \leq [^6]\text{Mn} \leq 0.04$ apfu). v) Phlogopite from perovskite magnetite ($0.02 \leq [^4]\text{Al} \leq 1.11$, $0.04 \leq [^4]\text{Fe} \leq 1.05$, $2.85 \leq [^4]\text{Si} \leq 3.01$, $2.19 \leq [^6]\text{Mg} \leq 2.76$, $0.01 \leq [^6]\text{Ti} \leq 0.06$, $0 \leq [^6]\text{Mn} \leq 0.02$ apfu) exhibits a chemical composition intermediate between mica crystals from glimmerite ($2.94 \leq [^4]\text{Si} \leq 3.03$, $0 \leq [^4]\text{Al} \leq 0.12$, $0.85 \leq [^4]\text{Fe} \leq 1.05$, $2.57 \leq [^6]\text{Mg} \leq 2.90$, $0.06 \leq [^6]\text{Fe} \leq 0.27$, $0 \leq [^6]\text{Ti} \leq 0.02$; $0 \leq [^6]\text{Mn} \leq 0.01$ apfu) and bebedourite (Brigatti *et al.* 1996b).

To sum up, the trioctahedral micas from the Tapira complex are generally characterized by low Al content, and Fe^{3+} is therefore commonly essential to fill the tetrahedral site (Fig. 1). The Al deficiency of micas has been interpreted in different ways. i) In the case of mica from lamproites and orangeites, it was interpreted as a consequence of the peralkalinity of the magma (Mitchell & Bergman 1991, Mitchell 1995). ii) According to Gibson *et al.* (1995), the Al-poor composition of most of the trioctahedral micas in mantle-derived rocks (*i.e.*, the formation of tetra-ferriphlogopite) can be attributed to the local post-emplacement environment of crystallization rather than to the composition of the parental magma. iii) The low Al-concentration in the liquid and high $f(\text{O}_2)$ were also recognized as factors for the formation of tetra-ferriphlogopite (*e.g.*, Arima & Edgar 1981, Heathcote & McCormick 1989, Brigatti *et al.* 1996b). iv) Recently, the crystallization of tetra-ferriphlogopite in a carbonatite-bearing alkaline-ultrabasic complex was attributed to the occurrence of oxidizing conditions during last stages of crystallization of the carbonatite (Krasnova 2001).

Greenwood (1998) indicated that the solubility of Ti in trioctahedral micas cannot be only related to parage-

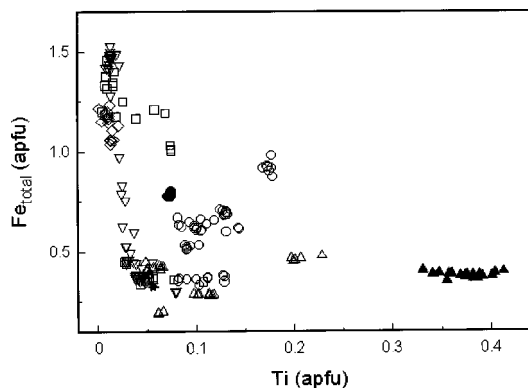


FIG. 2. Plot of Fe_{total} versus Ti (apfu) for trioctahedral micas from Alto Paranaíba Igneous Province. Trioctahedral micas from the Tapira Complex: crosses: dunite (Brigatti *et al.* 1996b); open circles: bebedourite (Brigatti *et al.* 1996b, and this study); open diamonds: glimmerite (Brigatti *et al.* 1996b); open triangles pointing down: perovskite magnetite (Brigatti *et al.* 1996b); open squares: garnet magnetite; filled circles: clinopyroxenite. Trioctahedral micas from Limeira I intrusion: open triangles pointing up. Trioctahedral micas from Presidente Olegario lavas: filled triangles pointing up.

netic constraints, but also to physicochemical conditions, prevailing during crystallization [*i.e.*, temperature and $f(\text{O}_2)$ increase, pressure decrease]. Despite the low Ti content of the trioctahedral micas at Tapira, there is a high availability of Ti in the liquid, as testified by the very high amounts of Ti-bearing phases (*i.e.*, perovskite, titaniferous magnetite, and schorlomite). Thus the varia-

TABLE 4. ATOM COORDINATES AND EQUIVALENT ISOTROPIC AND ANISOTROPIC (\AA^2) DISPLACEMENT FACTORS FOR THE CRYSTALS OF TRIOCTAHEDRAL MICA-1M STUDIED

| Atom | x/a | y/b | z/c | B_{eq} | β_{11}^* | β_{22}^* | β_{33}^* | β_{12}^* | β_{13}^* | β_{23}^* |
|-----------------|------------|------------|------------|----------|----------------|----------------|----------------|----------------|----------------|----------------|
| Sample Tpp16-6a | | | | | | | | | | |
| O1 | 0.0143(7) | 0 | 0.1698(4) | 1.55(8) | 0.0160(10) | 0.0046(4) | 0.0031(3) | 0 | 0.0009(5) | 0 |
| O2 | 0.3280(5) | 0.2277(3) | 0.1706(2) | 1.51(6) | 0.0124(8) | 0.0057(3) | 0.0030(2) | -0.0008(4) | 0.0014(3) | -0.0005(2) |
| O3 | 0.1299(4) | 0.1674(2) | 0.3910(2) | 0.63(4) | 0.0030(6) | 0.0015(2) | 0.0027(2) | 0.0003(3) | 0.0011(2) | -0.0001(2) |
| O4 | 0.1330(6) | 0.5 | 0.3976(3) | 0.55(6) | 0.0037(9) | 0.0010(3) | 0.0022(2) | 0 | 0.0004(4) | 0 |
| T | 0.0760(1) | 0.16674(9) | 0.22814(7) | 0.54(2) | 0.0032(2) | 0.0014(1) | 0.0020(1) | 0.0002(2) | 0.0005(1) | 0.0000(1) |
| M1 | 0 | 0 | 0.5 | 0.54(4) | 0.0029(6) | 0.0009(2) | 0.0025(2) | 0 | 0.0010(2) | 0 |
| M2 | 0 | 0.3322(2) | 0.5 | 0.52(2) | 0.0029(4) | 0.0010(1) | 0.0022(1) | 0 | 0.0004(2) | 0 |
| A | 0 | 0.5 | 0 | 2.37(5) | 0.0244(7) | 0.0076(2) | 0.0043(2) | 0 | 0.0014(3) | 0 |
| Sample Tax27-1 | | | | | | | | | | |
| O1 | 0.0158(5) | 0 | 0.1703(3) | 1.85(6) | 0.0210(10) | 0.0051(3) | 0.0032(2) | 0 | -0.0001(4) | 0 |
| O2 | 0.3265(4) | 0.2300(2) | 0.1697(2) | 1.91(5) | 0.0176(6) | 0.0068(2) | 0.0035(2) | -0.0018(3) | 0.0016(3) | -0.0008(2) |
| O3 | 0.1303(3) | 0.1669(2) | 0.3907(2) | 0.95(3) | 0.0079(5) | 0.0024(2) | 0.0027(1) | 0.0002(2) | 0.0004(2) | 0.0000(1) |
| O4 | 0.1324(4) | 0.5 | 0.3974(2) | 0.99(5) | 0.0080(7) | 0.0029(2) | 0.0026(2) | 0 | 0.0006(3) | 0 |
| T | 0.0758(1) | 0.16669(6) | 0.22744(6) | 0.41(1) | 0.0033(2) | 0.0010(1) | 0.0012(1) | 0.0000(1) | 0.0004(1) | 0.0000(1) |
| M1 | 0 | 0 | 0.5 | 0.65(3) | 0.0050(4) | 0.0013(1) | 0.0023(1) | 0 | 0.0008(2) | 0 |
| M2 | 0 | 0.3331(1) | 0.5 | 0.63(2) | 0.0042(2) | 0.0016(1) | 0.0021(1) | 0 | 0.0005(1) | 0 |
| A | 0 | 0.5 | 0 | 2.65(4) | 0.0270(5) | 0.0086(2) | 0.0047(1) | 0 | 0.0015(2) | 0 |
| Sample Taa11-1A | | | | | | | | | | |
| O1 | 0.0134(7) | 0 | 0.1699(4) | 1.40(8) | 0.0150(10) | 0.0020(3) | 0.0045(4) | 0 | 0.0009(5) | 0 |
| O2 | 0.3290(4) | 0.2284(3) | 0.1706(2) | 1.47(5) | 0.0125(8) | 0.0051(3) | 0.0033(2) | -0.0016(4) | 0.0020(3) | -0.0005(2) |
| O3 | 0.1302(3) | 0.1667(2) | 0.3904(2) | 0.51(4) | 0.0014(6) | 0.0023(2) | 0.0014(2) | 0.0003(3) | 0.0002(2) | 0.0000(2) |
| O4 | 0.1309(5) | 0.5 | 0.3962(3) | 0.56(6) | 0.0035(9) | 0.0019(3) | 0.0015(2) | 0 | 0.0001(4) | 0 |
| T | 0.0757(1) | 0.16666(9) | 0.22758(8) | 0.53(2) | 0.0023(2) | 0.0016(1) | 0.0020(1) | 0.0001(1) | 0.0006(1) | 0.0000(1) |
| M1 | 0 | 0 | 0.5 | 0.51(3) | 0.0019(4) | 0.0015(2) | 0.0020(1) | 0 | 0.0003(2) | 0 |
| M2 | 0 | 0.3327(1) | 0.5 | 0.53(2) | 0.0022(3) | 0.0015(1) | 0.0020(1) | 0 | 0.0001(1) | 0 |
| A | 0 | 0.5 | 0 | 2.54(4) | 0.0242(7) | 0.0084(2) | 0.0050(2) | 0 | 0.0016(3) | 0 |
| Sample Tai17-1 | | | | | | | | | | |
| O1 | 0.0109(4) | 0 | 0.1695(2) | 1.38(5) | 0.0158(8) | 0.0026(2) | 0.0032(2) | 0 | -0.0008(3) | 0 |
| O2 | 0.3290(3) | 0.2271(2) | 0.1697(2) | 1.37(4) | 0.0118(5) | 0.0043(2) | 0.0034(1) | -0.0020(3) | 0.0016(2) | -0.0006(1) |
| O3 | 0.1307(2) | 0.1669(1) | 0.3913(1) | 0.69(3) | 0.0058(4) | 0.0012(1) | 0.0025(1) | 0.0000(2) | 0.0006(2) | 0.0000(1) |
| O4 | 0.1322(4) | 0.5 | 0.3974(2) | 0.76(4) | 0.0059(6) | 0.0015(2) | 0.0026(2) | 0 | 0.0003(3) | 0 |
| T | 0.07585(9) | 0.16666(6) | 0.22742(5) | 0.71(1) | 0.0055(2) | 0.0013(1) | 0.0026(1) | 0.0000(1) | 0.0006(1) | 0.0000(1) |
| M1 | 0 | 0 | 0.5 | 0.71(2) | 0.0053(3) | 0.0010(1) | 0.0030(1) | 0 | 0.0010(1) | 0 |
| M2 | 0 | 0.33252(8) | 0.5 | 0.74(2) | 0.0048(2) | 0.0013(1) | 0.0030(1) | 0 | 0.0006(1) | 0 |
| A | 0 | 0.5 | 0 | 2.35(3) | 0.0227(4) | 0.0070(1) | 0.0051(1) | 0 | 0.0013(2) | 0 |
| Sample Ta9 | | | | | | | | | | |
| O1 | 0.0219(7) | 0 | 0.1690(3) | 1.38(8) | 0.0170(10) | 0.0032(4) | 0.0026(3) | 0 | -0.0005(5) | 0 |
| O2 | 0.3232(4) | 0.2330(3) | 0.1695(2) | 1.40(6) | 0.0116(8) | 0.0053(3) | 0.0027(2) | -0.0026(4) | 0.0014(3) | -0.0007(2) |
| O3 | 0.1306(4) | 0.1672(2) | 0.3905(2) | 0.62(4) | 0.0044(6) | 0.0019(2) | 0.0018(2) | 0.0000(3) | 0.0004(3) | 0.0000(2) |
| O4 | 0.1318(6) | 0.5 | 0.3963(3) | 0.66(7) | 0.0050(10) | 0.0015(3) | 0.0023(3) | 0 | 0.0005(4) | 0 |
| T | 0.0758(1) | 0.16671(8) | 0.22728(8) | 0.67(2) | 0.0049(2) | 0.0016(1) | 0.0022(1) | 0.0000(1) | 0.0005(1) | 0.0000(1) |
| M1 | 0 | 0 | 0.5 | 0.74(3) | 0.0049(4) | 0.0014(1) | 0.0029(1) | 0 | 0.0009(2) | 0 |
| M2 | 0 | 0.3331(1) | 0.5 | 0.75(2) | 0.0042(3) | 0.0020(1) | 0.0026(1) | 0 | 0.0007(1) | 0 |
| A | 0 | 0.5 | 0 | 2.70(5) | 0.0260(7) | 0.0091(2) | 0.0050(2) | 0 | 0.0015(3) | 0 |
| Sample Li12a | | | | | | | | | | |
| O1 | 0.0226(7) | 0 | 0.1709(3) | 1.58(7) | 0.0200(10) | 0.0031(3) | 0.0035(3) | 0 | 0.0016(5) | 0 |
| O2 | 0.3237(4) | 0.2331(3) | 0.1691(2) | 1.66(5) | 0.0128(7) | 0.0067(3) | 0.0033(2) | -0.0029(4) | 0.0018(3) | -0.0004(2) |
| O3 | 0.1295(3) | 0.1670(2) | 0.3908(2) | 0.48(3) | 0.0029(4) | 0.0011(2) | 0.0019(1) | 0.0001(2) | 0.0008(2) | 0.0001(1) |
| O4 | 0.1323(5) | 0.5 | 0.3968(2) | 0.44(5) | 0.0030(7) | 0.0010(2) | 0.0016(2) | 0 | 0.0006(3) | 0 |
| T | 0.0758(1) | 0.16668(7) | 0.22792(7) | 0.46(1) | 0.0022(2) | 0.0010(1) | 0.0019(1) | 0.0000(1) | 0.0006(1) | -0.0001(1) |
| M1 | 0 | 0 | 0.5 | 0.50(3) | 0.0023(4) | 0.0010(1) | 0.0023(1) | 0 | 0.0010(2) | 0 |
| M2 | 0 | 0.3333(1) | 0.5 | 0.63(2) | 0.0034(3) | 0.0015(1) | 0.0025(1) | 0 | 0.0010(1) | 0 |
| A | 0 | 0.5 | 0 | 2.58(4) | 0.0232(6) | 0.0089(2) | 0.0052(2) | 0 | 0.0015(2) | 0 |

TABLE 4 (continued). ATOM COORDINATES AND EQUIVALENT ISOTROPIC AND ANISOTROPIC (\AA^2) DISPLACEMENT FACTORS FOR THE CRYSTALS OF TRIOCTAHEDRAL MICA-1M STUDIED

| Atom | x/a | y/b | z/c | B_{eq} | β_{11}^* | β_{22}^* | β_{33}^* | β_{12}^* | β_{13}^* | β_{23}^* |
|-----------------|------------|------------|------------|-----------------|----------------|----------------|----------------|----------------|----------------|----------------|
| Sample Tpp16-6b | | | | | | | | | | |
| O1 | 0.0030(7) | 0 | 0.1701(3) | 1.95(8) | 0.0210(10) | 0.0058(4) | 0.0032(3) | 0 | -0.0011(5) | 0 |
| O2 | 0.3336(4) | 0.2234(3) | 0.1702(2) | 2.06(6) | 0.0202(8) | 0.0073(3) | 0.0034(2) | -0.0014(4) | 0.0023(3) | -0.0011(2) |
| O3 | 0.1304(3) | 0.1668(2) | 0.3909(2) | 0.64(3) | 0.0052(5) | 0.0013(2) | 0.0022(2) | 0.0001(3) | 0.0006(2) | 0.0000(1) |
| O4 | 0.1327(5) | 0.5 | 0.3978(2) | 0.60(5) | 0.0048(8) | 0.0016(2) | 0.0017(2) | 0 | 0.0004(3) | 0 |
| T | 0.0758(1) | 0.16661(6) | 0.22669(6) | 0.75(1) | 0.0059(2) | 0.0019(1) | 0.0023(1) | 0.0000(1) | 0.0007(1) | 0.0000(1) |
| M1 | 0 | 0 | 0.5 | 0.66(3) | 0.0046(4) | 0.0014(1) | 0.0024(1) | 0 | 0.0007(2) | 0 |
| M2 | 0 | 0.3327(1) | 0.5 | 0.65(2) | 0.0045(3) | 0.0013(1) | 0.0024(1) | 0 | 0.0008(1) | 0 |
| A | 0 | 0.5 | 0 | 2.22(3) | 0.0231(5) | 0.0070(2) | 0.0040(1) | 0 | 0.0016(2) | 0 |
| Sample Tpp16-6c | | | | | | | | | | |
| O1 | 0.0043(4) | 0 | 0.1700(2) | 1.89(5) | 0.0220(8) | 0.0058(2) | 0.0026(2) | 0 | -0.0004(3) | 0 |
| O2 | 0.3334(3) | 0.2236(2) | 0.1703(1) | 1.90(3) | 0.0192(5) | 0.0071(2) | 0.0027(1) | -0.0015(3) | 0.0015(2) | -0.0008(1) |
| O3 | 0.1300(2) | 0.1669(1) | 0.3911(1) | 0.59(2) | 0.0048(3) | 0.0014(1) | 0.0018(1) | 0.0003(1) | 0.0006(1) | 0.0000(1) |
| O4 | 0.1327(3) | 0.5 | 0.3983(2) | 0.61(3) | 0.0047(4) | 0.0018(2) | 0.0016(1) | 0 | 0.0004(2) | 0 |
| T | 0.07563(7) | 0.16664(4) | 0.22676(4) | 0.71(1) | 0.0062(1) | 0.0020(1) | 0.0019(1) | 0.0000(1) | 0.0007(1) | 0.0000(1) |
| M1 | 0 | 0 | 0.5 | 0.63(2) | 0.0048(2) | 0.0015(1) | 0.0020(1) | 0 | 0.0007(1) | 0 |
| M2 | 0 | 0.33267(7) | 0.5 | 0.63(1) | 0.0048(2) | 0.0015(1) | 0.0021(1) | 0 | 0.0007(1) | 0 |
| A | 0 | 0.5 | 0 | 2.28(2) | 0.0234(3) | 0.0077(1) | 0.0037(1) | 0 | 0.0012(1) | 0 |
| Sample Ma1 | | | | | | | | | | |
| O1 | 0.0322(5) | 0 | 0.1661(2) | 1.59(5) | 0.0216(9) | 0.0030(2) | 0.0033(2) | 0 | 0.0008(3) | 0 |
| O2 | 0.3164(3) | 0.2389(2) | 0.1650(2) | 1.65(4) | 0.0148(5) | 0.0058(2) | 0.0034(1) | -0.0028(3) | 0.0011(2) | -0.0005(2) |
| O3 | 0.1305(2) | 0.1680(2) | 0.3900(1) | 0.85(3) | 0.0086(4) | 0.0019(1) | 0.0025(1) | 0.0001(2) | 0.0010(2) | 0.0001(1) |
| O4 | 0.1308(4) | 0.5 | 0.4002(2) | 1.07(4) | 0.0090(6) | 0.0034(2) | 0.0027(2) | 0 | 0.0012(2) | 0 |
| T | 0.07455(9) | 0.16694(6) | 0.22406(5) | 0.61(1) | 0.0054(1) | 0.0011(1) | 0.0022(1) | 0.0001(1) | 0.0009(1) | 0.0000(1) |
| M1 | 0 | 0 | 0.5 | 0.63(2) | 0.0046(3) | 0.0009(1) | 0.0028(1) | 0 | 0.0014(2) | 0 |
| M2 | 0 | 0.3396(1) | 0.5 | 0.93(2) | 0.0053(2) | 0.0036(1) | 0.0026(1) | 0 | 0.0010(1) | 0 |
| A | 0 | 0.5 | 0 | 2.26(2) | 0.0203(4) | 0.0060(1) | 0.0064(1) | 0 | 0.0021(2) | 0 |

O: anionic sites; T: tetrahedral site; M: octahedral sites; A: interlayer site.

* $\exp[-(h^2\beta_{11} + \dots + 2hk\beta_{12} + \dots)]$. Labels a, b and c refer to different refined crystals from the same rock sample. Standard deviations are given in parentheses.

tion in Ti content in micas can be attributed both to the overall mineralogical association, including the presence of competing phases, and to the extreme conditions of $f(\text{O}_2)$, $a(\text{H}_2\text{O})$ and $f(\text{CO}_2)$ at the late stage of magmatic evolution. The higher temperature (Feeley & Sharp 1996) seems to be the most significant factor that controls Ti increase in micas from Presidente Olegario (Figs. 1b, 2).

In garnet magnetite rocks from Tapira complex (sample Tpp16-6, Table 2), mica presents a wide compositional variation, ranging from $^{[4]}\text{Fe}^{3+}$ -bearing phlogopite to ferroan tetra-ferriphlogopite. As suggested by Brod *et al.* (2001), this feature supports the metasomatic origin of ferroan tetra-ferriphlogopite as a result of the replacement of the original phlogopite.

Crystal chemistry

The compositional variation of the micas from the APiP complicates the description of the mechanisms governing the crystal chemistry of the layer. However, the main exchange-mechanisms which control the layer

topology seem to be homovalent substitutions $^{[4]}\text{Fe}^{3+}$ $^{[4]}\text{Al}^{3+}_{-1}$ and $^{[6]}\text{Fe}^{2+}$ $^{[6]}\text{Mg}^{2+}_{-1}$, and heterovalent exchange-vectors, such as $^{[6]}\text{Ti}^{4+}$ $^{[6]}\square$ $^{[6]}\text{Mg}^{2+}_{-2}$, $^{[6]}\text{Ti}^{4+}$ O_2 $^{[6]}\text{Mg}^{2+}_{-1}$ $(\text{OH})_{-2}$, $^{[6]}\text{(Mg, Fe)}^{2+}_{-1}$ $^{[4]}\text{Si}^{4+}_{-1}$ $^{[6]}\text{Fe}^{3+}$ $^{[4]}\text{Al}^{3+}$, and $^{[6]}\text{Fe}^{2+}_{-1}$ $(\text{OH})_{-1}$ $^{[6]}\text{Fe}^{3+}$ O^{2-} . Thus, changes in geometrical parameters may be related to compositional changes in both tetrahedral and octahedral sites.

The mean $\langle T\text{-O} \rangle$ bond distance is related to occupancy of the tetrahedral site by the regression equation $\langle T\text{-O} \rangle (\text{\AA}) = 1.607 + 4.201 \cdot 10^{-2} \cdot [^{[4]}\text{Al}^{3+}] + 7.68 \cdot 10^{-2} \cdot [^{[4]}\text{Fe}^{3+}]$ (Brigatti & Guggenheim 2000). Thus, the substitution $^{[4]}\text{Fe}^{3+}$ $^{[4]}\text{Al}^{3+}_{-1}$, which links phlogopite and tetra-ferriphlogopite, increases the dimensions of the tetrahedral site (Fig. 3a) and requires both the extension of the triads of octahedra (*i.e.*, the unshared edges of octahedra; Fig. 3b) and the increase in distortion of the ring of tetrahedra (*i.e.*, α ; Fig. 3c) to link the sheet of octahedra by the O3 oxygen atom. Differences between α values displayed by $^{[4]}\text{Fe}^{3+}$ -bearing phlogopite (sample Tpp16-6a; $\alpha = 8.6^\circ$) and ferroan $^{[4]}\text{Fe}^{3+}$ -bearing phlogopite (sample Ta9; $\alpha = 6.7^\circ$), both from garnet magnetite samples and with similar T-site occupancies

TABLE 5. SELECTED BOND-LENGTHS (Å) OBTAINED FROM STRUCTURE REFINEMENT OF THE TRIOCTAHEDRAL MICA-1M CRYSTALS STUDIED

| | Tpp16-6a | Tax27-1 | Taa11-1A | Tai17-1 | Ta9 | Lil2a | Tpp16-6b | Tpp16-6c | Mal |
|------------------------|----------|----------|----------|----------|----------|----------|----------|----------|----------|
| T-O1 | 1.666(2) | 1.665(1) | 1.663(2) | 1.667(1) | 1.663(2) | 1.653(1) | 1.677(1) | 1.676(1) | 1.646(1) |
| T-O2 | 1.658(3) | 1.666(2) | 1.663(2) | 1.663(2) | 1.658(2) | 1.663(2) | 1.676(2) | 1.677(2) | 1.649(2) |
| T-O2' | 1.667(3) | 1.666(2) | 1.657(2) | 1.668(2) | 1.661(2) | 1.657(2) | 1.675(2) | 1.675(2) | 1.644(2) |
| T-O3 | 1.653(2) | 1.658(2) | 1.647(2) | 1.661(2) | 1.652(1) | 1.648(2) | 1.668(2) | 1.670(1) | 1.652(2) |
| <T-O> | 1.661 | 1.664 | 1.657 | 1.665 | 1.658 | 1.655 | 1.674 | 1.674 | 1.648 |
| M1-O3 (×4) | 2.098(2) | 2.103(2) | 2.096(2) | 2.095(1) | 2.104(2) | 2.093(2) | 2.105(2) | 2.104(1) | 2.094(1) |
| M1-O4 (×2) | 2.057(3) | 2.066(2) | 2.069(3) | 2.061(2) | 2.069(3) | 2.061(2) | 2.065(2) | 2.065(2) | 2.043(2) |
| <M1-O> | 2.084 | 2.090 | 2.087 | 2.084 | 2.092 | 2.082 | 2.092 | 2.091 | 2.077 |
| M2-O3 (×2) | 2.080(2) | 2.098(2) | 2.092(2) | 2.087(2) | 2.095(2) | 2.088(2) | 2.099(2) | 2.096(1) | 2.119(2) |
| M2-O3' (×2) | 2.096(2) | 2.100(2) | 2.093(2) | 2.091(1) | 2.096(2) | 2.096(2) | 2.101(2) | 2.104(1) | 2.082(1) |
| M2-O4 (×2) | 2.068(2) | 2.067(2) | 2.067(2) | 2.066(2) | 2.069(2) | 2.060(2) | 2.072(2) | 2.070(1) | 1.983(2) |
| <M2-O> | 2.081 | 2.088 | 2.084 | 2.081 | 2.086 | 2.082 | 2.091 | 2.090 | 2.061 |
| A-O1 (×2) | 3.364(4) | 3.373(3) | 3.367(4) | 3.381(2) | 3.330(4) | 3.333(4) | 3.435(4) | 3.431(2) | 3.238(3) |
| A-O1' (×2) | 2.988(4) | 3.003(3) | 2.979(4) | 2.972(2) | 3.018(4) | 3.025(4) | 2.950(3) | 2.958(2) | 3.026(3) |
| A-O2 (×4) | 3.379(3) | 3.364(2) | 3.374(3) | 3.382(2) | 3.329(3) | 3.320(3) | 3.435(3) | 3.434(2) | 3.226(2) |
| A-O2' (×4) | 2.985(3) | 3.005(2) | 2.985(2) | 2.974(2) | 3.026(3) | 3.016(3) | 2.955(2) | 2.958(2) | 3.026(2) |
| <A-O> _{inner} | 2.986 | 3.004 | 2.983 | 2.973 | 3.024 | 3.019 | 2.953 | 2.958 | 3.026 |
| <A-O> _{outer} | 3.374 | 3.367 | 3.371 | 3.382 | 3.329 | 3.324 | 3.435 | 3.433 | 3.230 |

T: tetrahedral site, M: octahedral sites, A: interlayer site. Standard deviations are given in parentheses. Nature of the trioctahedral micas: Tpp16-6a: $^{44}\text{Fe}^{2+}$ -bearing phlogopite; Tax27-1, Taa11-1A, Tai17-1, Ta9 and Lil2a: ferroan $^{44}\text{Fe}^{3+}$ -bearing phlogopite; Tpp16-6b, Tpp16-6c: ferroan tetra-ferriphlogopite; Mal: titanian phlogopite.

(*i.e.*, with similar values of $X_{\text{tetra-ferriphlogopite}}$ content [= $100 \times 4 [^{44}\text{Fe}^{3+} / (^{44}\text{Si}^{4+} + \text{Al}^{3+} + \text{Fe}^{3+})]$], can be related to differences in the level of Fe^{2+} in octahedral sites, which produced a relatively large sheet of octahedra in the ferroan phlogopite crystal.

In ferroan tetra-ferriphlogopite, the tetrahedrally coordinated cation approaches the ideal position at the center of the polyhedron, whereas in $^{44}\text{Fe}^{3+}$ -bearing phlogopite, ferroan $^{44}\text{Fe}^{3+}$ -bearing phlogopite and titanian phlogopite, the tetrahedrally coordinated cation is shifted toward the O3 oxygen atom (*i.e.*, toward the apex of the tetrahedra) and the basal edges of the tetrahedra reduce in length (Fig. 4). This reduction further adjusts the lateral dimensions of the sheets, and so the ring of tetrahedra deviates less from hexagonal symmetry. In tetra-ferriphlogopite, the misfit between sheets of octahedra and sheets of tetrahedra, produced by the increase of the $\langle \text{O} - \text{O} \rangle_{\text{basal}}$ length, in addition to α rotation, is compensated by an increase in the mean length of the unshared edges of the octahedra (Table 6). In end-member phlogopite, the mean value of the unshared edge is 3.051 Å (Hazen & Burnham 1973), whereas in end-member tetra-ferriphlogopite, it increases to 3.097 Å (Brigatti *et al.* 1996a). Thus the $^{60}\text{Fe}^{2+}$ -for- ^{60}Mg exchange in ferroan tetra-ferriphlogopite does not seem to produce important differences in the geometry of the sheet of octahedra because the octahedra mainly reflect the topology of the tetrahedra instead of the local crystal chemistry.

In the crystals from the Tapira Complex, the mean electron density (m.e.d.) at both M1 and M2 sites increases with $^{60}\text{Fe}^{2+}$ $^{60}\text{Mg}^{2+}$ exchange. This behavior is similar to that displayed by trioctahedral true micas of the phlogopite-annite join [*i.e.*, the m.e.d. of both M1 and M2 sites increases from phlogopite to annite through ferroan phlogopite and magnesian annite; a regression equation on 63 crystals: m.e.d._{M1} (e^-) = $0.72 + 0.964$ m.e.d._{M2}; regression coefficient $r = 0.979$; Brigatti & Guggenheim 2000]. On the contrary, for intermediate compositions between phlogopite and annite, exchange vectors that introduce cations of different charge (or vacancies) in octahedral sites affect significantly differences in mean bond-length between M1 and M2 sites, suggesting a partial ordering of octahedrally coordinated cations. In the trioctahedral micas of the Tapira complex, the difference ($\Delta \langle M-O \rangle$) between $\langle M1-O \rangle$ and $\langle M2-O \rangle$ mean bond-distances is less than 0.006 Å (thus $\Delta \langle M-O \rangle \leq 3\sigma$, where σ is the estimated standard deviation on the mean value). Thus, the nearly equal size and mean electron-density between M1 and M2 suggest disorder among octahedrally coordinated cations. Note that crystals taken from the same rock type (*e.g.*, trioctahedral micas from garnet magnetite and bebedourite), with different octahedral occupancies, as well as ferroan tetra-ferriphlogopite, confirm the presence of disorder among octahedral cations (Fig. 5). On the other hand, titanian phlogopite from the Presidente Olegario lavas shows evidence of cation ordering, with the mean bond-

TABLE 6. SELECTED PARAMETERS TO DESCRIBE TETRAHEDRA, OCTAHEDRA AND INTERLAYER, DERIVED FROM STRUCTURE REFINEMENT OF THE TRIOCTAHEDRAL MICA-1M CRYSTALS STUDIED

| | Tpp16-6a | Tax27-1 | Taa11-1A | Tai17-1 | Ta9 | Lil2a | Tpp16-6b | Tpp16-6c | Mal |
|--|----------|---------|----------|---------|--------|--------|----------|----------|--------|
| Parameters to describe the tetrahedra | | | | | | | | | |
| α (°) | 8.6 | 7.9 | 8.5 | 9.0 | 6.7 | 6.7 | 10.5 | 10.4 | 4.5 |
| Δz (Å) | 0.0077 | 0.0060 | 0.0067 | 0.0013 | 0.0057 | 0.0177 | 0.0011 | 0.0026 | 0.0107 |
| τ (°) | 110.7 | 110.5 | 110.4 | 110.6 | 110.7 | 110.8 | 110.0 | 110.1 | 110.8 |
| Volume (Å ³) | 2.351 | 2.361 | 2.336 | 2.367 | 2.340 | 2.324 | 2.406 | 2.409 | 2.295 |
| $\langle O-O \rangle_{\text{basal}}$ (Å) | 2.696 | 2.701 | 2.696 | 2.702 | 2.691 | 2.683 | 2.727 | 2.726 | 2.666 |
| Thickness (Å) | 2.264 | 2.266 | 2.248 | 2.268 | 2.259 | 2.256 | 2.267 | 2.269 | 2.270 |
| T_{disp} (Å) | 0.0364 | 0.0324 | 0.0301 | 0.0319 | 0.0360 | 0.0409 | 0.0186 | 0.0189 | 0.0335 |
| Parameters to describe the octahedra | | | | | | | | | |
| ψ_{M1} (°) | 58.65 | 58.66 | 58.53 | 58.73 | 58.62 | 58.59 | 58.76 | 58.83 | 59.25 |
| ψ_{M2} (°) | 58.60 | 58.63 | 58.48 | 58.68 | 58.53 | 58.58 | 58.75 | 58.81 | 58.99 |
| Volume $_{M1}$ (Å ³) | 11.90 | 12.00 | 11.96 | 11.88 | 12.03 | 11.87 | 12.02 | 12.00 | 11.72 |
| Volume $_{M2}$ (Å ³) | 11.85 | 11.97 | 11.91 | 11.84 | 11.95 | 11.86 | 12.00 | 11.98 | 11.47 |
| $e_u M1$ (Å) | 3.083 | 3.092 | 3.083 | 3.085 | 3.093 | 3.078 | 3.098 | 3.099 | 3.092 |
| $e_s M1$ (Å) | 2.805 | 2.814 | 2.814 | 2.802 | 2.817 | 2.805 | 2.812 | 2.808 | 2.774 |
| $e_u M2$ (Å) | 3.077 | 3.088 | 3.078 | 3.080 | 3.083 | 3.077 | 3.096 | 3.097 | 3.060 |
| $e_s M2$ (Å) | 2.803 | 2.812 | 2.812 | 2.800 | 2.813 | 2.804 | 2.811 | 2.808 | 2.763 |
| Thickness (Å) | 2.168 | 2.175 | 2.179 | 2.163 | 2.178 | 2.170 | 2.170 | 2.165 | 2.124 |
| Parameters to describe the interlayer | | | | | | | | | |
| Thickness (Å) | 3.455 | 3.449 | 3.441 | 3.440 | 3.427 | 3.437 | 3.454 | 3.461 | 3.295 |
| $\Delta(A-O)$ (Å) | 0.388 | 0.363 | 0.388 | 0.409 | 0.305 | 0.305 | 0.482 | 0.475 | 0.204 |

Nature of the trioctahedral micas: Tpp16-6a: ⁴¹Fe³⁺-bearing phlogopite; Tax27-1, Taa11-1A, Tai17-1, Ta9 and Lil2a: ferroan ⁴¹Fe³⁺-bearing phlogopite; Tpp16-6b, Tpp16-6c: ferroan tetra-ferriphlogopite; Mal: titanium phlogopite.

Note: α (tetrahedral rotation angle) = $\sum_{i=1}^6 \frac{\alpha_i}{6}$ where $\alpha_i = |120^\circ - \phi_i|/2$ and where ϕ_i is the angle between basal edges of neighboring tetrahedra articulated in the ring. $\Delta z = [Z_{(\text{O}_{\text{basal}})_{\text{max}}} - Z_{(\text{O}_{\text{basal}})_{\text{min}}}] [\text{csin}\beta]$. τ (tetrahedral flattening angle) = $\sum_{i=1}^3 \frac{(\text{O}_{\text{basal}} - \hat{T} - \text{O}_{\text{basal}})_i}{3}$. $T_{\text{disp}} = \sqrt{\left(\frac{(\text{T} - \text{O}_{\text{basal}})}{3}\right)^2 - \left(\frac{(\text{O} - \text{O})_{\text{basal}}}{3}\right)^2 - \frac{(\text{T} - \text{O}_{\text{apical}})}{3}}$. ψ (octahedral flattening angle) = $\cos^{-1} \frac{\text{octahedral thickness}}{2(M-O)}$ (Donnay *et al.* 1964). e_u and e_s are the unshared and shared edges of octahedra, respectively. $\Delta(A-O) = (A-O)_{\text{outer}} - (A-O)_{\text{inner}}$.

distance $\langle M1-O \rangle$ greater than $\langle M2-O \rangle$ ($\Delta \langle M-O \rangle = 0.016$ Å) and with the mean electron-density at *M2* higher than that at *M1*. Both features suggest a preference of heavy and smaller cations for the *M2* site (Table 7). In Ti-bearing crystals from the APIP suite, the *M2*-O4 bond length decreases as Ti content increases, thus indicating a displacement of Ti from the geometric center of the octahedron. The interlayer separation (and therefore the *A*-O4 bond distance) decreases as well. These features indicate a stronger attraction of the O4 oxygen atom toward the interlayer cation (*A*) and *M2* cations. Furthermore, deprotonation of O4 would be expected (Fig. 6). Our results differ from those expected by Foley (1990), who identified the exchange vector $^{[6]}\text{Ti}^{4+} [^{[6]}\square] [^{[6]}\text{Mg}^{2+}]_2$ as the main mechanism for Ti incorporation into the trioctahedral micas. Our results suggest that Ti^{4+} in phlogopite and ferroan phlogopite occurs nearly entirely *via* a Ti-oxy exchange mecha-

nism (*i.e.*, $^{[6]}\text{Ti}^{4+} \text{O}_2 [^{[6]}\text{Mg}^{2+}]_1 (\text{OH})_2$). Feeley & Sharp (1996) pointed out that the H₂ released by dehydrogenation reactions can combine with O₂ in the melt, thus increasing the volatile components and the explosive nature of volcanism. Thus the presence of a high amount of Ti at the *M2* sites of phlogopite from Presidente Olegario lavas would be required to maintain the local charge on deprotonated O4-O4 edges. In *M2* polyhedra, O4 positions are on adjacent corners in *cis* orientation, whereas in *M1* polyhedra, they are on opposite corners, in *trans* orientation (Bailey 1994). Ti ordering at *M2* could be required to limit the repulsion among the deprotonated oxygen atoms and thus to prevent the breakdown of the structure.

The unit-cell parameters *a* and *b* increase from phlogopite to tetra-ferriphlogopite and therefore correlate strongly with $^{[4]}\text{Fe}^{3+}$ content (Fig. 7). In contrast, the *c* parameter decreases mostly with Ti content (Fig. 8).

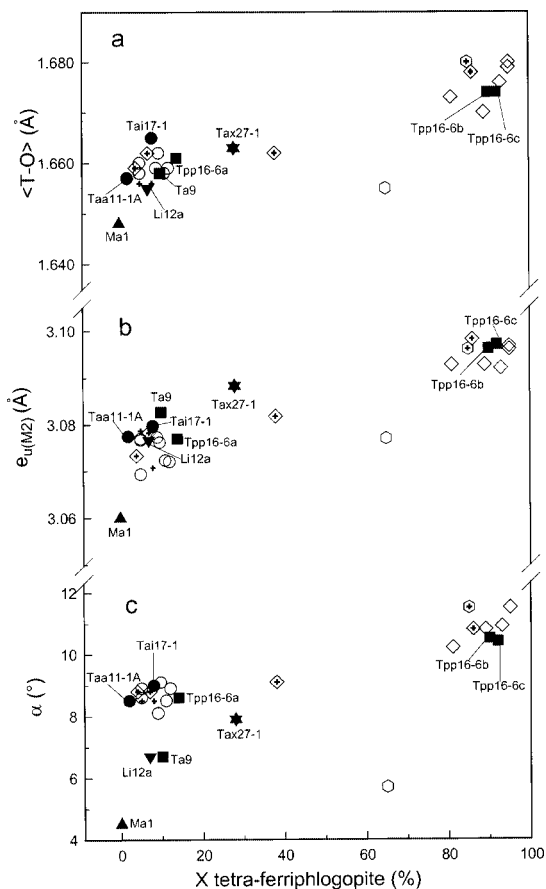


FIG. 3. a) Mean $\langle T-O \rangle$ bond-distance versus $X_{\text{tetra-ferriphlogopite}}$. b) Mean proportion of unshared edges at the M2 site ($e_{\text{u}}(\text{M2})$) versus $X_{\text{tetra-ferriphlogopite}}$. c) Tetrahedron rotation angle, α , versus the proportion of the tetra-ferriphlogopite end member ($X_{\text{tetra-ferriphlogopite}}$). Filled symbols refer to trioctahedral micas from this study, whereas open symbols refer to trioctahedral mica crystals from Brigatti *et al.* (1996a, b, 1999). Samples from the Tapira complex: crosses: dunite, circles: bebedourite, diamonds enclosing a cross: perovskite magnetite, diamonds: glimmerite, squares: garnet magnetite, star: clinopyroxene. Titanian phlogopite from Presidente Olegario lavas: triangle pointing up, ferroan $^{44}\text{Fe}^{3+}$ -bearing phlogopite from Limeira I: triangle pointing down, tetra-ferriphlogopite of Hazen *et al.* (1981): hexagon, tetra-ferriphlogopite of Semenova *et al.* (1977): hexagon enclosing a cross.

Thus, the variation in lateral unit-cell parameters reflects the in-plane increase in the dimension of the sheet of tetrahedra, whereas the c value decreases as the interlayer separation and the $M-O4$ distance diminish.

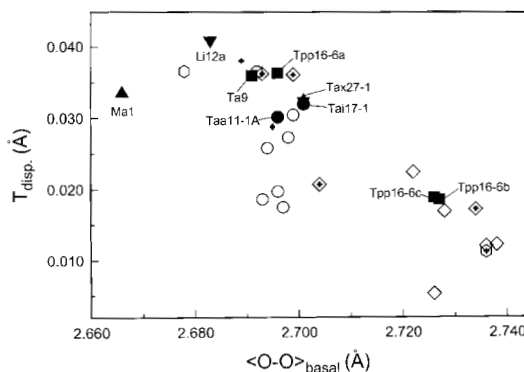


FIG. 4. Displacement of the tetrahedrally coordinated cation from its ideal position (T_{disp}) versus the mean basal edge-length $\langle O-O \rangle_{\text{basal}}$. Symbols as in Figure 3. T_{disp} is defined in Table 6.

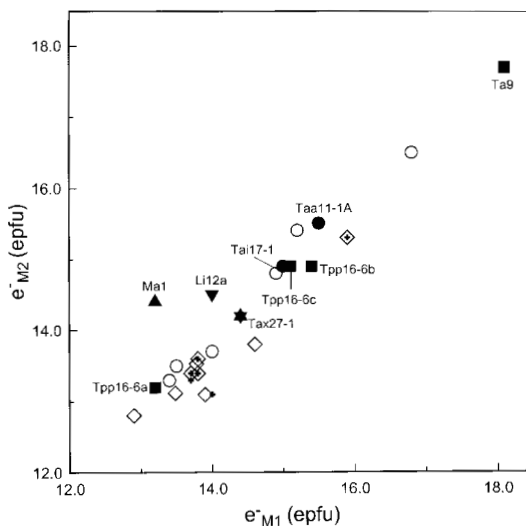


FIG. 5. Number of electrons per formula unit at the M2 site versus the number of electrons per formula unit at the M1 site. Symbols as in Figure 3.

ACKNOWLEDGEMENTS

We thank R.M. Hazen, R. Martin, R.T. Downs and two anonymous referees for comments on the manuscript. This work was supported by Ministero dell'Università e della Ricerca Scientifica of Italy (Project: "Layer silicates: Crystal chemical, structural and petrological aspects") and by Consiglio Nazionale delle Ricerche (CNR) of Italy. Centro Interdipartimentale Grandi Strumenti (CIGS) of the University of Modena and Reggio Emilia is acknowledged for the use of the

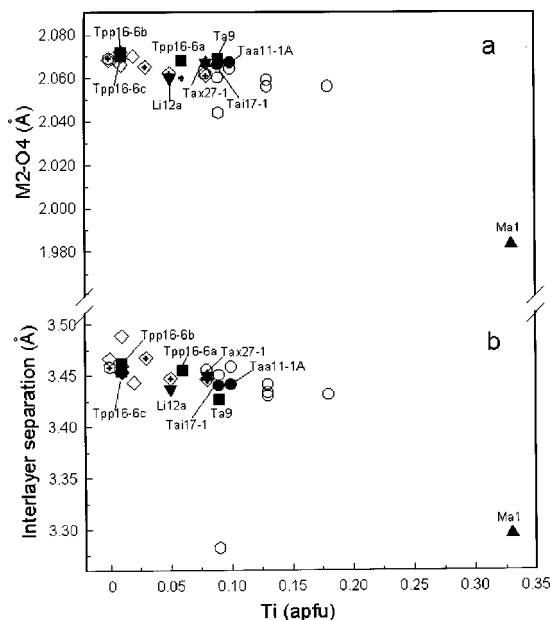


FIG. 6. a) M2–O4 basal length versus Ti content; b) interlayer separation versus Ti content. Symbols as in Figure 3.

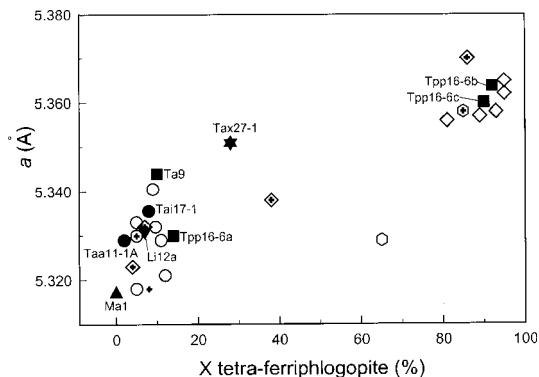


FIG. 7. Variation in unit-cell parameter a versus $X_{\text{tetra-ferriphlogopite}}$. Symbols as in Figure 3.

single-crystal diffractometer. The Italian CNR is also acknowledged for maintaining the electron microprobe at the Department of Earth Sciences, University of Modena and Reggio Emilia.

REFERENCES

ARAÚJO, D.P. & GASPAR, J.C. (1993): Fe^{3+} no sítio tetraédrico de flogopitas das rochas do complexo carbonatítico de

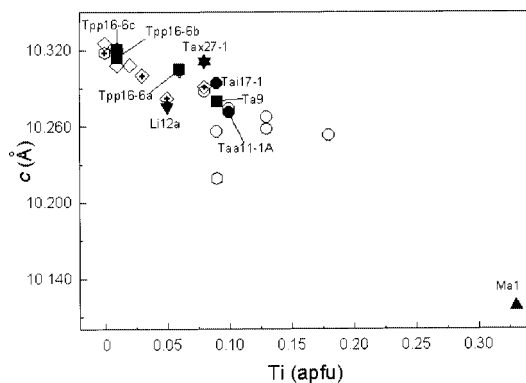


FIG. 8. Variation in unit-cell parameter c versus Ti content. Symbols as in Figure 3.

Catalão I, Brasil. *Proc. 4th Congresso Brasileiro de Geoquímica (Brasília), Extended Abstr.*, 62–63.

ARIMA, M. & EDGAR, A.D. (1981): Substitution mechanisms and solubility of titanium in phlogopites from rocks of probable mantle origin. *Contrib. Mineral. Petrol.* **77**, 288–295.

BAILEY, S.W. (1984): Crystal chemistry of the true micas. In *Micas* (S.W. Bailey, ed.). *Rev. Mineral.* **13**, 13–60.

BRIGATTI, M.F. & GUGGENHEIM, S. (2000): Mica crystal chemistry and the influence of intensive variables on atomistic models. *Advances on Micas (Problems, Methods, Applications in Geodynamics)*. Accademia Nazionale dei Lincei, Roma, Italy (29–56).

_____, LALONDE, A.E. & MEDICI, L. (1999): Crystal chemistry of $^{44}\text{Fe}^{3+}$ -rich phlogopites: a combined single-crystal X-ray and Mössbauer study. In *Clays for our Future* (H. Kodama, A.R. Mermut & J.K. Torrance, eds.). *Proc. 11th Int. Clay Conf. (Ottawa, 1997)*, 317–327.

_____, LUGLI, C., POPPI, L., FOORD, E.E. & KILE, D.E. (2000): Crystal chemical variations in Li- and Fe-rich micas from Pikes Peak batholith (central Colorado). *Am. Mineral.* **85**, 1275–1286.

_____, MEDICI, L. & POPPI, L. (1996a): Refinement of the structure of natural ferriphlogopite. *Clays Clay Minerals* **44**, 540–545.

_____, _____, SACCANI, E. & VACCARO, C. (1996b): Crystal chemistry and petrologic significance of Fe^{3+} -rich phlogopite from the Tapira carbonatite complex, Brazil. *Am. Mineral.* **81**, 913–927.

BROD, J.A., GASPAR, J.C., ARAÚJO, D.P., GIBSON, S.A., THOMPSON, R.N. & JUNQUEIRA-BROD, T.C. (2001): Phlogopite and tetra-ferriphlogopite from Brazilian carbonatite complexes: petrogenetic constraints and implications for mineral-chemistry systematics. *J. Asian Earth Sci.* **19**, 265–296.

TABLE 7. REFINED AND CALCULATED SITE-OCCUPANCY (*epfu*) FOR THE TRIOCTAHEDRAL MICA-1M CRYSTALS STUDIED

| | Tpp16 -6a | Tax27 -1 | Taa11 -1A | Tai17 -1 | Ta9 | Li12a | Tpp16 -6b | Tpp16 -6c | Mal |
|---|--------------|-------------|--------------|-------------|---------|---------|--------------|--------------|---------|
| <i>M1</i> octahedral site | | | | | | | | | |
| Fe ²⁺ | 0.09 | 0.22 | 0.25 | 0.21 | 0.43 | 0.13 | 0.24 | 0.21 | 0.27 |
| Mg | 0.91 | 0.73 | 0.75 | 0.79 | 0.57 | 0.87 | 0.75 | 0.79 | 0.51 |
| Vacancy | | 0.05 | | | | | 0.01 | | 0.22 |
| man _{calc} | 13.3 | 14.5 | 15.5 | 14.9 | 18.0 | 13.8 | 15.2 | 14.9 | 13.1 |
| man _{XREF} | 13.2(1) | 14.4(1) | 15.5(1) | 15.0(1) | 18.1(1) | 14.0(1) | 15.4(1) | 15.1(1) | 13.2(1) |
| <i>M2</i> octahedral site | | | | | | | | | |
| Ti | 0.03 | 0.04 | 0.05 | 0.05 | 0.05 | 0.03 | 0.01 | 0.01 | 0.16 |
| Fe ³⁺ | | | | | | | | | 0.02 |
| Fe ²⁺ | 0.06 | 0.13 | 0.21 | 0.17 | 0.37 | 0.16 | 0.19 | 0.20 | 0.04 |
| Mg | 0.91 | 0.83 | 0.74 | 0.78 | 0.58 | 0.81 | 0.80 | 0.79 | 0.78 |
| man _{calc} | 13.1 | 14.2 | 15.4 | 14.9 | 17.7 | 14.5 | 14.8 | 14.9 | 14.4 |
| man _{XREF} | 13.2(1) | 14.2(1) | 15.5(1) | 14.9(1) | 17.7(1) | 14.5(1) | 14.9(1) | 14.9(1) | 14.4(1) |
| man(<i>M1</i> +2 <i>M2</i>) _{calc} | 39.5 | 42.9 | 46.4 | 44.7 | 53.4 | 42.9 | 44.8 | 44.7 | 42.0 |
| man(<i>M1</i> +2 <i>M2</i>) _{XREF} | 39.6 | 42.7 | 46.4 | 44.6 | 53.4 | 43.0 | 45.1 | 44.8 | 42.0 |
| man(<i>M1</i> +2 <i>M2</i>) _{EPMA} | 39.5 | 42.9 | 46.4 | 44.6 | 53.4 | 42.7 | 44.6 | 44.6 | 42.0 |
| Interlayer <i>A</i> site | | | | | | | | | |
| man(<i>A</i>) _{XREF} | 18.6(1) | 18.1(1) | 18.9(1) | 19.6(1) | 20.0(1) | 18.1(1) | 19.4(1) | 19.7(1) | 20.0(1) |
| man(<i>A</i>) _{EPMA} | 18.7 | 18.4 | 18.8 | 19.4 | 19.7 | 18.5 | 19.6 | 19.6 | 19.8 |

Note: XREF: X-ray refinement, EPMA: electron-microprobe analysis, calc: calculated using EPMA and XREF results, man: mean atomic number. Labels a, b, c refer to different refined crystals from the same rock sample. Values in parentheses represent the estimated standard deviation. Nature of the trioctahedral micas: Tpp16-6a: ¹⁴Fe³⁺-bearing phlogopite; Tax27-1, Taa11-1A, Tai17-1, Ta9 and Li12a: ferroan ¹⁴Fe³⁺-bearing phlogopite; Tpp16-6b, Tpp16-6c: ferroan tetra-ferriphlogopite; Mal: titanian phlogopite.

- _____, GIBSON, S.A., THOMPSON, R.N., JUNQUEIRA-BROD, T.C., SEER, H.J., MORAES, L.C. & BOAVENTURA, G.R. (2000): Kamafugite affinity of the Tapira alkaline-carbonatite complex (Minas Gerais, Brazil). *Rev. Brasil. Geociências* **30**, 404-408.
- BUSING, W.R., MARTIN, K.O. & LEVI, H.S. (1962): ORFLS, a Fortran crystallographic least-square program. *U.S. Nat. Tech. Inform. Serv. ORNL-TM-305*.
- DONNAY, G., MORIMOTO, N., TAKEDA, H. & DONNAY, J.D.H. (1964): Trioctahedral one-layer micas. I. Crystal structure of a synthetic iron mica. *Acta Crystallogr.* **17**, 1369-1373.
- DONOVAN, J.J. (1995): *PROBE: PC-Based Data Acquisition and Processing for Electron Microprobes*. Advanced Microbeam, 4217 King Graves Rd., Vienna, Ohio 44473, U.S.A.
- FEELEY, T.C. & SHARP, Z.D. (1996): Chemical and hydrogen isotope evidence for in situ dehydrogenation of biotite in silicic magma chambers. *Geology* **24**, 1021-1024.
- FOLEY, S.F. (1989): Experimental constraints on phlogopite chemistry in lamproites. 1. The effect of water activity and oxygen fugacity. *Eur. J. Mineral.* **1**, 411-426.
- _____. (1990): Experimental constraints on phlogopite chemistry in lamproites. 2. The effect of pressure-temperature variations. *Eur. J. Mineral.* **2**, 327-341.
- GASPAR, J.C. (1989): *Géologie et minéralogie du complexe carbonatitique de Jacupiranga, Brésil*. Thèse de doctorat, Univ. d'Orléans, Orléans, France.
- _____, SILVA, A.J.G.C. & ARAÚJO, D.P. (1994): Composition of priderite in phlogopites from the Catalão I carbonatite complex, Brazil. *Mineral. Mag.* **58**, 409-415.
- _____ & WYLLIE, P.J. (1987): The phlogopites from the Jacupiranga carbonatite intrusions. *Mineral. Petrol.* **36**, 121-134.
- GIBSON, S.A., THOMPSON, R.N., LEONARDOS, O.H., DICKIN, A.P. & MITCHELL, J.G. (1995): The Late Cretaceous impact of the Trindade mantle plume: evidence from large-volume, mafic, potassic magmatism in SE Brazil. *J. Petrol.* **36**, 189-229.
- GIULI, G., PARIS, E., WU, Z., BRIGATTI, M.F., CIBIN, G., MOTTANA, A. & MARCELLI, A. (2001): Experimental and theoretical XANES and EXAFS study of tetra-ferriphlogopite. *Eur. J. Mineral.* (in press).

- GREENWOOD, J.C. (1998): Barian-titanian micas from Ilha da Trindade, South Atlantic. *Mineral. Mag.* **62**, 687-695.
- HAZEN, R.M. & BURNHAM, C.W. (1973): The crystal structures of one-layer phlogopite and annite. *Am. Mineral.* **58**, 889-900.
- _____, FINGER, L.W. & VELDE, D. (1981): Crystal structure of a silica- and alkali-rich trioctahedral mica. *Am. Mineral.* **66**, 586-591.
- HEATHCOTE, R.C. & MCCORMICK, G.R. (1989): Major cation substitution in phlogopite and evolution of carbonatite in the Potash Sulfur Springs complex, Garland County, Arkansas. *Am. Mineral.* **74**, 132-140.
- KRASNOVA, N.I. (2001): The Kovdor phlogopite deposit, Kola Peninsula, Russia. *Can. Mineral.* **39**, 33-44.
- MEYROWITZ, R. (1970): New semimicroprocedure for determination of ferrous iron in refractory silicate minerals using a sodium metafluoborate decomposition. *Anal. Chem.* **42**, 1110-1113.
- MITCHELL, R.H. (1995): *Kimberlites, Orangeites and Related Rocks*. Plenum Press, New York, N.Y.
- _____, & BERGMAN, S.C. (1991): *Petrology of Lamproites*. Plenum Press, New York, N.Y.
- MOLER, C. (1992): *The Student Edition of MATLAB*. The Math Works Inc., Prentice Hall, Englewood Cliff, New Jersey.
- NORTH, A.C.T., PHILLIPS, D.C. & MATHEWS, F.S. (1968): A semi-empirical method of absorption correction. *Acta Crystallogr.* **A24**, 351-359.
- SEMENOVA, T.F., ROZHDESTVENSKAYA, I.V. & FRANK-KAMENETSKII, V.A. (1977): Refinement of the crystal structure of tetraferriphlogopite. *Sov. Phys. Crystallogr.* **22**, 680-683.
- SIEMENS (1993): *XSCANS System - Technical reference Siemens Analytical X-ray Instruments*.
- Received February 8, 2001, revised manuscript accepted July 31, 2001.*